



On the tuning of plateaus in atmospheric and oceanic ^{14}C records to derive calendar chronologies of deep-sea cores and records of ^{14}C marine reservoir age changes

5 Edouard Bard¹ and Timothy J. Heaton²

1 CEREGE, Aix-Marseille University, CNRS, IRD, INRAE, Collège de France,
Technopôle de l'Arbois, Aix-en-Provence, France

10 2 School of Mathematics and Statistics, University of Sheffield, Sheffield S3 7RH, UK

15 **Abstract:** As an extended comment on the paper by Sarnthein et al. (2020), we express strong reservations about the methodology of the so-called ^{14}C plateau tuning (PT) technique used to date marine sediment records and its implications on the determination of ^{14}C marine reservoir ages (MRA).

The main problems are linked to: the assumption of constant MRA during ^{14}C -age
20 plateaus; the lack of consideration of foraminifera abundance changes coupled to bioturbation that can create spurious plateaus in marine sediments; the assumption that plateaus have the same shapes and durations in atmospheric and oceanic records; the implication that atmospheric $^{14}\text{C}/^{12}\text{C}$ peaked instantaneously from one plateau to the next; that the ^{14}C plateaus represent 82% of the total time spent between 14,000 and 29,000 cal yr BP, whereas during the remaining
25 18% of the time, the radiocarbon clock was running almost 5 times too fast; that the sparsity, combined with the level of analytical uncertainties and additional noise, in both atmospheric and marine data do not currently allow one to reliably or robustly identify plateaus (should they exist) beyond 15,000 cal yr BP; and that the determination and identification of plateaus is reliant upon significant changes in sedimentation rate within the marine sediments which are,
30 a priori, unknown and are not verified with an independent method.

The concerns we raise are supported and strengthened with carbon cycle box-model experiments and statistical simulations of pseudo-atmospheric and pseudo-marine records, allowing us to test the ability to identify and tune ^{14}C -age plateaus, in the context of noisy and sparse data.

35



1/ Introduction

40 Sarnthein et al. (2020) review the results of a technique based on tuning hypothesized
 ^{14}C -age plateaus they inferred in deep sea sediment cores with those that they have proposed in
the atmospheric radiocarbon calibration curve, notably using the Lake Suigetsu record (Bronk
Ramsey et al. 2012, 2020). The proposed outcomes of the so-called ‘Plateau Tuning’ (PT) are
to establish accurate and precise calendar age scales of the marine sediments and, at the same
45 time, to determine the ^{14}C marine reservoir ages (MRAs) at the sea surface (for ^{14}C measured
on planktonic foraminifera) and ventilation ages of deeper water masses (using ^{14}C measured
on benthic foraminifera).

Sarnthein et al. (2020) reviews the results obtained by PT published over the last 13
years by the Kiel group (Sarnthein et al. 2007, 2011, 2013, 2015, Balmer et al. 2016, Sarnthein
50 & Werner 2017, Balmer & Sarnthein 2018, Küssner et al. 2018). By comparing the records
from many locations, the authors conclude in section 2.2 that the ^{14}C -age plateaus beyond
15,000 cal yr BP “*show little coherence*” with independent ^{10}Be records based on polar ice
cores and therefore that the cause of these ^{14}C anomalies may not be linked to cosmogenic
production changes.

55 The authors thus propose that extremely large and variable ventilation ages may be the
causes of these ^{14}C -age plateaus, constituting the fingerprint of abrupt reversals of deep ocean
circulation and abrupt release or drawdown of CO_2 into or from the atmosphere. Nevertheless,
the authors admit that “*ocean models still poorly reproduce*” their reconstruction of deep ocean
circulation and carbon cycle changes (end of abstract). They claim that this mismatch is due to
60 model deficiencies in spatial resolution and tuning with reference data.

We have strong reservations about the appropriateness of the PT technique and
consequently also the reliability of the results obtained in Sarnthein et al. (2020). The PT
technique, proposed and used by the same authors from Kiel for more than 13 years, has not
been checked and replicated independently by other groups. Only Umling & Thunell (2017)
65 used the PT technique, but found rather puzzling results (see more in section 2.3). PT has been
presented on several occasions during International Radiocarbon Conferences and workshops
of the IntCal group, but has never been adopted as a viable technique to reconstruct past ^{14}C
variations (Reimer et al. 2020, Heaton et al. 2020a and previous IntCal iterations by Reimer et
al. 2009, 2013).

70 The review paper by Sarnthein et al. (2020) only compiles previous papers by the same
group. The risk is to mislead readers into thinking that the PT technique is now firmly



established. Indeed, the compiled records based on PT leads to perplexing outcomes (no coherence with either production changes or with ocean modeling results). This failure is linked to the inherent pitfalls listed below, which are not treated adequately in Sarnthein et al. (2020), nor in former papers by the same group.

75 With this extended comment, our objective is to expose and discuss openly some of the inherent problems linked to PT. We split our discussion into two sections. Firstly, we present our concerns from a geoscientific perspective; Secondly, we provide our statistical concerns with the proposed PT method and provide illustrative examples that highlight its intrinsic
80 difficulties.

2/ Paleoclimatic & paleoceanographic perspective

2.1/ The PT principle is reminiscent of the ‘¹⁴C wiggle matching technique’ used to refine the dating of large pieces of wood with multiple ¹⁴C analyses over a tree-ring sequence of at least a few decades (Bronk Ramsey et al. 2001). However, Sarnthein et al. (2020) propose to do this with ocean sediments, that are not annually laminated, and to obtain calendar chronologies accurate and precise at the “decadal-to-centennial” level mentioned in their section 1.1. However, there is no independent constraint on the sedimentation rate variations in these ocean cores (without annual varves). Indeed, sedimentation rate changes linked to climatic-oceanographic events (e.g. Dansgaard-Oeschger and Heinrich events) or more local sedimentological causes could also create ¹⁴C-age plateaus.

2.2/ In addition to determining the calendar chronology of ocean sediments, PT is also used to calculate, at the same time, a variable offset with the atmospheric ¹⁴C curve. The offset for planktonic foraminifera is often very large (1000-2000 ¹⁴C yrs), and is interpreted as being due to ¹⁴C reservoir age changes at the sea surface. However, in order to perform PT the authors are required to assume that the marine ¹⁴C reservoir age (MRA) is strictly constant during the age plateaus, which represent 82% of the total time spent between 14,000 and 29,000 cal yr BP. This assumption of reservoir age stability during ¹⁴C-age plateaus is antithetical with the conclusion that these plateaus are linked to carbon cycle changes. Such significant carbon cycle changes would have left their imprint in ¹⁴C records (Bard 1988), maybe even as ¹⁴C-age plateaus solely recorded in marine sediments. Hence, the ¹⁴C structures identified by Sarnthein et al. (2020) in pelagic sediments are severely under-constrained in ¹⁴C and calendar ages.

105 Indeed, changes in marine ¹⁴C reservoir age may either mask (or create false) plateaus



110 in the marine core causing issues with tuning to the atmospheric plateau. On the one hand, a decrease in MRA coinciding with an atmospheric ^{14}C -age plateau (i.e. a decrease in atmospheric $\Delta^{14}\text{C}$) may create a set of marine ^{14}C observations lacking any plateau. On the other, an increase in MRA may make a period where the atmospheric ^{14}C record does not plateau (e.g. constant atmospheric $\Delta^{14}\text{C}$) appear as a plateau in marine ^{14}C observations. In both these instances, PT will fail. Unless MRA only changes at the boundary times of their chosen plateau, identifying whether a potential plateau in a set of marine observations should be tuned to an atmospheric plateau is potentially confounded by the very changes to MRA the authors report.

115

2.3/ Sarnthein et al. (2020) refers to the ^{14}C calibration curve as a ‘rung ladder’ that is the basis of PT. Actually, the series of ^{14}C -age plateaus hypothesized by Sarnthein et al. (2020) resembles a ‘staircase’ more than a ‘rung ladder’. In Figure 1, we have created a Lake Suigetsu-only calibration curve using the same Bayesian statistical method used for IntCal20 (Heaton et al., 2020b, Reimer et al. 2020) but constructed based only upon the observations from Lake Suigetsu with its updated timescale (Bronk Ramsey et al. 2020). Fig. 1 shows the Lake Suigetsu ^{14}C data and the resulting Suigetsu-only radiocarbon calibration curve for the period beyond the last 14,000 cal yr BP (14 cal kyr BP) covered with high-precision data on tree-rings. Superimposed horizontal lines indicate the 15 hypothesized atmospheric ^{14}C -age plateaus of Sarnthein et al. (2020), with their numbering as listed in their Table 1. Fig. 2 is equivalent to Fig. 1, but compares the ^{14}C -age plateaus directly with the IntCal20 calibration curve (Reimer et al. 2020) which, in addition to Lake Suigetsu, uses (atmosphere-adjusted) ^{14}C determinations from speleothems, lacustrine and marine sediments, and corals; as well as some ^{14}C determinations obtained from floating tree-ring sequences. Besides the well-known plateau #1 corresponding to the beginning of the Bölling period, evidence for many of the older plateaus hypothesized by Sarnthein et al. (2020) is dubious. They are not replicated in either our statistically-robust Lake Suigetsu-only curve (Fig. 1) or the IntCal20 curve (Fig. 2). The weak evidence for many of these hypothesized ^{14}C -age plateaus is further detailed in section 3.1.

135 By focusing only on the plateaus, Sarnthein et al. (2020) overlook the implication that, in their model, ^{14}C ages must jump, often instantaneously, from one plateau to the next (i.e. like in a staircase as shown in Figs. 1 and 2). This is particularly true for five steps between 10 plateaus (10b to 10a, 9 to 8, 6b to 6a, 5b to 5a and 2b to 2a) for which the calendar gaps correspond to **zero** cal yr, but the atmospheric ^{14}C ages drops by between 340 and 750 ^{14}C yrs. Five other steps have also minimal calendar durations (70 to 170 cal yr) between 10 plateaus



140 (11 to 10b, 8 to 7, 7 to 6b, 6a to 5b and 5a to 4), but show large ^{14}C drops ranging from 660 to
1380 ^{14}C yr. Consequently, the total duration of ^{14}C plateaus represent 82% of the time spent
between 14 and 29 cal kyr BP, whereas during the remaining 18% of the time, the radiocarbon
clock was running almost 5 times too fast. The implication of the hypothetical staircase shape
of the atmospheric calibration curve, is that radiocarbon would have never behaved as a
145 geochronometer driven by regular radioactive decay.

It is useful to convert Figs. 1 and 2 in terms of $\Delta^{14}\text{C}$ in order to assess the implications
of these vertical steps. This is done in Fig. 3 which shows that ^{14}C -age plateaus are transformed
into triangular $\Delta^{14}\text{C}$ wiggles. The consequence of abrupt ^{14}C -age drops between ^{14}C -age
plateaus is that most $\Delta^{14}\text{C}$ wiggles exhibit instantaneous rises ranging between 50 to 250 %.

150 There is no known mechanism that could be responsible for such abrupt and large
asymmetric wiggles of the atmospheric $\Delta^{14}\text{C}$. Instantaneous ^{14}C production increases, that
result in about 4 times the average production in a year, were discovered recently (Miyake et
al. 2012, Mekhaldi et al. 2015), but the size of these spikes attributed to extreme solar particle
events is an order of magnitude smaller in terms of $\Delta^{14}\text{C}$ than that required to explain the jumps
155 between the hypothesized ^{14}C -age plateaus of Sarnthein et al. (2020). Furthermore, there is no
evidence of huge corresponding spikes in the ice core ^{10}Be record (Adolphi et al. 2018). In
addition, the impact of abrupt changes of the geomagnetic field were found to be negligible on
the production of ^{14}C (Fournier et al. 2015). Finally, it is unlikely that abrupt changes of the
carbon cycle are responsible for such large, frequent and very abrupt $\Delta^{14}\text{C}$ spikes. For example,
160 switching down the deep ocean circulation instantaneously in a carbon cycle box-model, leads
to a rather slow and limited $\Delta^{14}\text{C}$ rise in the atmosphere over several centuries (e.g. see Fig. 4b
by Goslar et al. 1995 or Fig. 5 by Hughen et al. 1998; see also simulations performed with more
complex models by Marchal et al. 2001, Delaygue et al. 2003, Ritz et al. 2008, Singarayer et
al. 2008). Consequently, the PT underlying assumption that the radiocarbon calibration curve
165 has the shape of a staircase, is in conflict with our basic understanding of ^{14}C as a tracer.

2.4/ Unfortunately, the Sarnthein et al. (2020) review paper fails to show a single figure
illustrating oceanic ^{14}C records with their plateaus compared, and tuned, with the atmospheric
calibration ^{14}C curve. It is thus necessary to dig into the literature to see the marine core records:
170 Figs. 3, 4 in Sarnthein et al. (2007) for cores SO17940, MD01-2416, ODP893A and PS2644,
Fig. 2 in Sarnthein et al. (2011) for core MD01-2378, Figs. 3 to 13 in Sarnthein et al. (2015)
for cores GIK23074, PS2644, MD08-3180, ODP1002, MD01-2378, GIK17940, SO50-37,
MD01-2416, MD02-2489, ODP893A, MD02-2503, Suppl. Figs. S1a,b,c,d in Balmer et al.



(2016) for cores GeoB1711-4, GeoB3910-1, KNR-159-5-36GGC, MD07-3076), Fig. 4 in
175 Sarnthein & Werner (2017) for cores GIK23258, MSM5/5-712, and T88-2, Fig. 2 in Balmer
& Sarnthein (2018) for core MD08-3180, Fig. 4 in Küssner et al. (2018) for core PS75-104-1.

Looking at these graphs is absolutely crucial to assess the poor quality of the
determination of ^{14}C -age plateaus in these ocean cores and their tuning to the atmospheric ^{14}C
calibration curve. This is particularly important as the PT implies sedimentation rates that vary
180 by up to a factor of 5 to 8 within a single core (e.g. cores PS2644 and MD08-3180 in Sarnthein
et al. 2015; PS75/104-1 in Küssner et al. 2018) and even much more, by orders of magnitude,
in other cores from the Nordic Seas (Sarnthein & Werner 2017).

In Appendix B of their Supplemental Information, Sarnthein et al. (2020) provide
summary Figures for 18 individual deep-sea cores, showing the final reconstructions of surface
185 and deep reservoir ages versus time for each core. However, these graphs are not really useful
to assess PT tuning because they do not show the raw ^{14}C data versus depth compared to the
Suigetsu ^{14}C record.

In fact, changes of sedimentation rates implied by PT are even larger than mentioned
above because remaining conflicts between atmospheric and marine ^{14}C records are resolved
190 by introducing ad-hoc discontinuities in the core stratigraphies. These periods forced to have a
sedimentation rate dropping down to zero are assumed to be sedimentological hiatuses
previously unnoticed (e.g. 9 hiatuses are inferred by PT in the 18 sediment cores presented in
Fig. S2). Sarnthein et al. (2020) further claim that the *«plateau-based high-resolution
chronology has led to the detection of numerous millennial-scale hiatuses overlooked by
conventional methods of stratigraphic correlation. In turn, the hiatuses give intriguing new
195 insights into past changes of bottom current dynamics linked to different millennial-scale
geometries of overturning circulation and climate change»*. No independent sedimentological
evidence is presented to verify these previously unnoticed hiatuses, which occur surprisingly at
the ^{14}C plateau boundaries for no obvious reason. These discontinuities may just be artefacts of
200 the PT method.

Surprisingly, the figure summarizing results on four South Pacific cores (Fig. S2c on
PS75-104, MD07/3088, SO213-76 and PS97/137-1) has been changed between the submitted
version (Fig. S4c available in *Climate of the Past Discussions*) and the final published paper by
Sarnthein et al. (2020). The changes are particularly important for the last two cores: for
205 example, the LGM surface reservoir age around 20 cal kyr BP has been divided by a factor two
for core PS97/137-1 (more than 2000 ^{14}C yr in the submitted version instead of 1000 ^{14}C yr in
the published version). Benthic reservoir ages have also changed by more than 1000 ^{14}C yr (up



or down) in the last two cores. In addition, both records now exhibit two hiatuses in the final publication as opposed to a single hiatus presented in the initial submission. Whatever the reasons for these changes, the reader cannot assess their validity by looking at these summary figures.

Outside the 18 records obtained by the Kiel group and compiled by Sarnthein et al. (2020), there is one further paper by other authors who have used PT for stratigraphical purposes and for reconstructing ^{14}C reservoir ages. Umling & Thunell (2017) used eyeball PT to derive their chronology for a sediment core located at 2.7 km depth in the Eastern Equatorial Pacific. The tuning of the ^{14}C record of core TRI163-23 onto the Suigetsu ^{14}C record, implies the unexpected presence of hiatuses in this core at boundaries between ^{14}C plateaus (i.e. gaps between plateaus #1a and YD, and between plateaus #2a and 1, see Fig. 3c of Umling & Thunell, 2017). The first hiatus is particularly long (1200 cal yr), but no independent data is presented to confirm the presence of such a large unconformity in this core. In addition, the deglacial ^{14}C reservoir ages reconstructed for core TRI163-23 exhibit discrepancies with the record obtained by de la Fuente et al. (2015) on another core from the Eastern Equatorial Pacific collected at a similar depth (2.9 km).

2.5/ The PT technique is focused on the detection and use of ^{14}C -age plateaus. This implies that a large part of the ^{14}C record is left unused in the matching process. This is actually surprising because plateaus are used in the frame of PT to define the absolute chronology of the marine sediment core, while plateaus in the ^{14}C calibration curve are generally viewed as poor periods for obtaining precise calibrated ages, in contrast to ‘high-slope’ parts of the calibration curve (e.g. Svetlik et al. 2019). The only potential justification we can identify for such an approach would be if one believed that changes to MRA could only occur at plateau boundaries (and remained otherwise constant). However, there is no special significance in the plateaus of the ^{14}C calibration curve. After transformation to atmospheric $\Delta^{14}\text{C}$ (Fig. 3), a ^{14}C -age plateau is only the second part of a wiggle, during which the $\Delta^{14}\text{C}$ decrease compensates the radioactive decay. If anything, the entire $\Delta^{14}\text{C}$ wiggle is the feature that should be matched (equivalent to a ‘high-slope’ – ‘low-slope’ sequence in the plot of ^{14}C age vs calendar age).

Without a clear justification for why plateau boundaries would coincide with all MRA changes, there is thus no reason to match the ^{14}C -age plateaus only and discard the other parts of the ^{14}C sequence. Matching the entire ^{14}C record with the target curve would mimic the wiggle matching technique used for tree sequences (without resolving the remaining pitfalls of having no independent calendar dating for most ocean sediments; and that no matching could



be done unless one already knew the MRA). Matching the entire ^{14}C sequence is also the method used to synchronize floating tree-ring sequences to a master chronology (e.g. Capano et al. 2020 used for the IntCal20 curve by Reimer et al. 2020).

245 Indeed, even if MRA changes were to occur only at plateau boundaries the marine and atmospheric ^{14}C -age records should show entirely the same shape, just with piecewise constant offsets during and between each plateau. This would provide an even stronger argument that the whole ^{14}C record should be matched. Plateau tuning would then reduce to finding the change points in the piecewise constant MRA offset between atmospheric and marine ^{14}C -ages.

250

2.6/ In contrast to the atmospheric ^{14}C calibration curve, there is indeed a special significance in a ^{14}C -age plateau observed in ocean sediments. As mentioned above, within a sediment core, a ^{14}C -age plateau could be a simple consequence of an abrupt sedimentation rate increase or even a slump that mixes sediments of the same age. Another potential source of ^{14}C -age plateaus has been completely overlooked by Sarnthein et al. (2020): the coupling of
255 continuous bioturbation with changes in the abundance of the ^{14}C signal carrier. Indeed, the assemblages of foraminifera used for ^{14}C analyses often varied in the past due to global or regional paleoceanographic conditions (these large and systematic faunal changes are the basis for the use of planktonic foraminifera in paleothermometry, e.g. Imbrie & Kipp 1971, Kucera et al. 2005).

260

 In particular, an abrupt decrease or an abrupt increase of the foraminifera abundance will inevitably create a ^{14}C -age plateau, as theorized by Broecker et al. (1984). The first demonstration was provided by Bard et al. (1987) who showed that ^{14}C -age plateaus and $\delta^{18}\text{O}$ phase lags measured on two planktonic species in a deep-sea core from the North Atlantic could
265 be explained quantitatively by bioturbation modeling forced with the abundance records of both species. Since 1987 many other groups have made similar observations of ^{14}C -age plateaus explained by bioturbation coupled with foraminifera abundance changes (e.g. Costa et al. 2017, Ausin et al. 2019).

270

 In order to interpret ^{14}C -age plateaus in ocean sediments, it is thus indisputably
270 necessary to show the absolute abundance records of the different foraminifera used for ^{14}C dating (counts expressed in number per gram of sediment). This has never been the case for any of the PT papers by the Kiel group used for this new compilation (Sarnthein et al. 2007, 2011, 2013, 2015, Balmer et al. 2016, Sarnthein & Werner 2017, Balmer & Sarnthein 2018, Küssner et al. 2018, Sarnthein et al. 2020), implying that several marine ^{14}C -age plateaus could be mere
275 sedimentary artefacts.



2.7/ Let us now assume that ^{14}C -age plateaus in marine records do match those identified in the atmospheric record (i.e. the basic assumption of the PT technique). What remains problematic, if we are intending to use PT to create a precise calendar age time scale for the marine record, is that marine ^{14}C -age plateaus are assumed to be as sharp and as long as atmospheric plateaus, even in the case of very large surface reservoir ages reconstructed by the method. The sections below show that this conflicts with our understanding of the carbon cycle.

For the past 14 kyr, high resolution ^{14}C data on tree-ring and ^{10}Be on polar ice cores have shown that most centennial $\Delta^{14}\text{C}$ wiggles in the atmosphere are due to cosmogenic production changes (Beer et al. 1988, Adolphi et al. 2016, 2017, 2018) mainly linked to the solar variability as illustrated by studies covering the last millennium (e.g. Bard et al. 1997, Muscheler et al. 2000, Delaygue & Bard 2011). This ^{14}C production signal is transferred from the atmosphere to the ocean surface before being slowly transported to the deep ocean. The atmospheric ^{14}C wiggle inevitably gets damped in the other reservoirs of the carbon cycle, notably the surface ocean. In addition, the oceanic wiggle is not strictly in phase with the atmospheric one. Both damping and phasing effects conflict with the main assumption of the PT technique, namely that marine ^{14}C -age plateaus can be matched directly to atmospheric ones.

Using numerical models, it is possible to quantify the damping and phasing effects, which depend directly on the duration of the $\Delta^{14}\text{C}$ wiggle and on the carbon residence time in the considered carbon cycle reservoir (or chain of reservoirs). A convenient way is to consider a sinusoidal production leading to attenuated and shifted signals in the atmosphere and the ocean surface (see Figure 4). The Indo-Pacific low-latitude surface box of the 12-box model by Bard et al. (1997) has a ^{14}C reservoir age of 320 ^{14}C yrs at steady state. The relative attenuation is a factor of 1.8 for 500-cal-yr long ^{14}C wiggles and a factor of 3.1 for 200-cal-yr long wiggles (amplitude in the troposphere divided by the amplitude in the surface ocean). The phase lag between atmospheric and oceanic response also varies with the duration of the ^{14}C production signal: about 60 and 45 cal yr for 500 and 200-cal-yr long wiggles, respectively.

To illustrate the relative attenuation increase with a larger reservoir age it is useful to consider the simulation for the Southern Ocean surface box which has a reservoir age of 890 ^{14}C yrs in the 12-box model. For the same 500-cal-yr and 200-cal-yr long $\Delta^{14}\text{C}$ wiggles, the relative attenuation factors are 3.0 and 3.4, respectively. Fig. 4a shows the results of these calculations for signal periods ranging from 2000 to 100 calendar yrs. The period is equivalent



310 to the duration of the $\Delta^{14}\text{C}$ wiggle and to twice the duration of the ^{14}C -age plateau, which corresponds to the descending part of the $\Delta^{14}\text{C}$ wiggle.

As illustrated in Fig. 4b, a 500-cal-yr long wiggle of cosmogenic production varying by $\pm 15\%$ around its mean value is sufficient to produce an atmospheric ^{14}C -age plateau. However, in the surface ocean boxes, the slope of the ^{14}C -age vs cal-age curves does not drop to zero, i.e.
315 there is absence of a ^{14}C -age plateau in the modelled surface ocean environment despite the atmospheric plateau. This is a direct consequence of the damping of ^{14}C signals by the carbon cycle.

The ^{14}C bomb spike of the early 1960s provides further evidence of the smoothing and phasing effects. The main ^{14}C injection lasted only a few years and the bomb spike can be
320 viewed as the impulse response function of the carbon cycle. In detail, the bomb pulse is complicated because the $\Delta^{14}\text{C}$ decrease observed in the atmosphere over the last 50 years is also partially due to the Suess effect linked to the input of anthropogenic CO_2 devoid of ^{14}C (Levin & Hesshaimer 2016). In any case, the ocean surface $\Delta^{14}\text{C}$ increased in the 1970s by 150-200 ‰ above pre-bomb values, which is about 5 times less than the maximum anomaly in the
325 atmospheric pool. This large damping effect remains true even for the shallowest lagoons (Grottoli & Akin 2007), which illustrates the efficacy of ocean mixing to counterbalance air-sea gas exchange.

Today the ocean surface $\Delta^{14}\text{C}$ is still above these pre-bomb values (e.g. Andrews et al. 2016) and this anomaly will remain with us for many decades to come as the present level in
330 the ocean surface is only about halfway through its long-term asymptotic decrease. The calculation of an average phase lag between atmosphere and ocean is difficult because the impulse response functions are completely asymmetric (i.e. the delay for the signal rise is totally different to that observed for the signal decrease). To sum up, the bomb spike in the surface ocean is also a century scale event, with an attenuation compatible with that calculated by
335 considering sinusoidal signals (Fig. 4a), which remains the traditional way used in signal analysis (i.e. so-called Bode plots).

2.8/ The considerations above apply to $\Delta^{14}\text{C}$ wiggles linked to ^{14}C production changes, but it has likewise been suggested that ^{14}C -age plateaus may also correspond to carbon cycle
340 changes, notably at the end of the Younger Dryas climatic event (Oeschger et al. 1980, Goslar et al. 1995, Hughen et al. 1998). This YD ^{14}C -age plateau may have been caused by an abrupt resumption of the meridional overturning circulation as simulated by numerical models (Goslar et al. 1995, Stocker & Wright 1996,1998, Hughen et al. 1998; see Fig. 17 by Bard 1998



345 comparing the ^{14}C -age plateau simulated by the 12-box model and the Bern 2.5D physical model).

In such a case, the ^{14}C perturbation originates from the ocean and the relative attenuation and phase relationships with the atmospheric pool are more complex, exhibiting regional differences. The surface ocean regions responsible for uptake or outgassing of CO_2 exhibit large effects with no delay, whereas other regions are only affected in a passive way through the atmosphere. For those widespread passive regions, we must refer back to the calculations shown in Figs. 4a,b, which lead to large attenuations in the ocean.

350 The study of atmosphere and surface ocean ^{14}C wiggles linked to spatially variable ocean-atmosphere exchange is inherently more complex as it requires spatial resolution with 2D-3D models and consideration of regional ^{14}C data to identify active and passive regions. However, regional gradient changes of surface ^{14}C simulated by models are generally on the order of a few centuries (Stocker & Wright 1998, Delaygue et al. 2003, Butzin et al. 2005, Franke et al. 2008, Singarayer et al. 2008, Ritz et al. 2008), rather than the millennia advocated by Sarnthein et al. (2020).

360 **2.9/** In the introductory section 1.2 of their paper, Sarnthein et al. (2020) mention a completely different method to reconstruct MRA based on ^{14}C datings of the same volcanic ash layer in land and marine sediments. This is indeed a precise and accurate method used in many studies including those cited by Sarnthein et al. (2020). However, they should have also cited the two seminal papers on the subject: Bard (1988) was the first to propose specifically the use of volcanic ash layers to reconstruct past MRA variations, and Bard et al. (1994) the first to reconstruct past MRA changes with this powerful method.

3/ Statistical perspective

370 **3.1/** From a statistical viewpoint, fundamental to the accuracy, robustness and reliability in the estimates of both the timescales and MRA obtained by PT, is whether true ^{14}C -age plateaus can be consistently identified and also matched between sparsely sampled and noisy records. In the case of marine sediment cores, identification of these ^{14}C -age plateaus is further confounded by potential MRA changes, bioturbation and the lack of an independent timescale. One needs to have confidence that the plateaus identified in both the marine and atmospheric ^{14}C records are not only genuine but have also been correctly tied together.



Sarnthein et al. (2020) do not appear to address this issue – instead concentrating on an argument as to whether the true underlying atmospheric ^{14}C record contain plateaus. This is a necessary condition, and is discussed further in Section 3.8, but certainly not sufficient for the reliability of PT. Rather, the main statistical concern for PT is as to whether any such genuine atmospheric ^{14}C -age plateaus can be identified in both the sparse, and uncertain, Lake Suigetsu ^{14}C record **and** the marine sediment ^{14}C record being plateau-tuned. If one either mislocates a true ^{14}C -age plateau in one or other of the records; or incorrectly pairs plateaus between records then the subsequent timescales of the sediment core and MRA estimation record will be unreliable. We thus raise the following specific statistical concerns:

3.2/ The PT technique is based on marine ^{14}C records with a limited amount of noisy data, leading to rather ambiguous estimations of the locations, and durations, of ^{14}C -age plateaus in ocean sediments. This is also true for the atmospheric ^{14}C -age plateaus that Sarnthein et al. (2020) hypothesize from the Lake Suigetsu and Hulu ^{14}C records (see Sarnthein et al.'s Fig. S1, showing ^{14}C error bars at 1σ).

Sarnthein et al. (2020) invoke ad-hoc changes of the dead carbon fraction (DCF) of the Hulu Cave speleothems (section 2.2), and an argument that filtering has removed the plateaus within the speleothem ^{14}C record, to explain the lack of correspondence between the ^{14}C -age plateaus they outline in both target curves (section 1.2). There is no obvious reason that would explain systematic changes in the speleothem DCF occurring only **during** the atmospheric ^{14}C -age plateaus in such a way as to both mask these atmospheric plateaus in the speleothem ^{14}C record, and to ensure that the speleothem record does not generate additional spurious, DCF-driven, ^{14}C -age plateaus between the genuine atmospheric ones. As already underlined in our section 2.2, the opposite hypothesis is made by Sarnthein et al. (2020) for MRA which is assumed to remain constant during the atmospheric ^{14}C -age plateaus, changing only at boundary times between plateaus.

Based on the comparison with the precise IntCal13 record over the past 14 cal kyr BP, the DCF for Hulu is in the order of 450 ± 70 ^{14}C yr (1σ , Cheng et al., 2018). This mean value and standard deviation have been further tested and refined in the frame of IntCal20, to give an estimate of 480 ± 55 ^{14}C yr (Reimer et al. 2020, Heaton et al. 2020b), by comparing the Hulu data for individual speleothems with the tree-ring ^{14}C record over the past 14 cal kyr BP. The low value and stability of the DCF are attributed to the characteristics of the Hulu cave with its sandstone ceiling and open system conditions with the soil above it. In a way similar to the ocean modeled in section 2.7, the carbon transport and mixing processes leading to the DCF



should have somewhat smoothed the atmospheric ^{14}C variations. Although a specific modeling should be performed for a particular cave system, the DCF value for Hulu cave (ca. 480 ^{14}C yr) is equivalent to the typical MRA of low-to-mid-latitude surface oceans. Consequently, the ^{14}C -age plateaus should be smoothed and delayed at a similar level as in surface ocean records, for which Sarnthein et al. (2020) assume that plateaus are of the same duration and timing as in the atmospheric record.

Further, one would expect that due to the time-directional nature of any speleothem filtering (i.e. that it averages over past atmospheric ^{14}C values) ^{14}C -age plateaus in the Hulu record should either be seen with a time lag compared with the atmosphere, or at least towards the more recent end of the atmospheric plateau. This is not the case in Sarnthein et al. (2020) where Figure S1 predominantly proposes Hulu Cave ^{14}C -age plateaus that occur at the beginning (i.e. older end) of their hypothesized atmospheric ^{14}C -age plateaus.

When one considers the uncertainty in the ^{14}C determinations (see Fig. S1 of Sarnthein et al. (2020) showing error bars plotted at 1σ), it is unclear how strong the evidence for several of the hypothesized atmospheric ^{14}C -age plateaus is. When measurement uncertainties are large, one would expect (simply due to the randomness of these uncertainties) to observe sequences of ^{14}C determinations that are non-monotonic even when the underlying atmospheric ^{14}C -age to calendar age is monotonically increasing. Based upon the Lake Suigetsu observations and uncertainties, it is therefore hard to assess whether some of the hypothesized atmospheric ^{14}C -age plateaus really exist or are rather just random artefacts due to measurement uncertainty. This is particularly true for the upper panel of their Fig. S1 focused on the period between 21 and 27 cal kyr BP.

To illustrate this concern about the reliability of the hypothesized plateaus more clearly, as mentioned in section 2.3, we have created a Lake Suigetsu-only calibration curve using the same Bayesian statistical method used for IntCal20 (Heaton et al., 2020b, Reimer et al. 2020) but constructed based only upon the observations from Lake Suigetsu (using the updated Lake Suigetsu calendar age timescale provided by Bronk Ramsey et al. 2020). Fig. 1 shows the Lake Suigetsu ^{14}C data with their 1σ analytical uncertainties (both in radiocarbon and calendar age) and the resulting Suigetsu-only radiocarbon calibration curve with its 95% posterior predictive probability interval. Superimposed horizontal lines indicate the 15 hypothesized atmospheric plateaus with their numbering as listed in Table 1 of Sarnthein et al. (2020). Besides the well-known plateau #1 corresponding to the beginning of the Bölling period, it is dubious as to whether many of the older plateaus in particular are supported by the Lake Suigetsu data based on our statistical assessment.



445 Furthermore, most of the hypothesized plateaus have calendar durations exceeding the
95% posterior predictive probability interval around the Lake Suigetsu data (notably plateaus
2a, 4, 8 and 10b). The two plateaus (# 2b and 6b) with the shortest duration (410 cal yrs) are
compatible with the probability interval around the Lake Suigetsu data. However, these sections
of the calibration curve are also compatible with straight oblique lines with no plateau at all.
450 Such a conclusion is supported by Fig. 2 comparing the plateaus and the IntCal20 curve. Only
a few plateaus could correspond to particular structures of the IntCal20 curve, notably plateau
1 which is already known, and maybe plateaus # 7, 10a and 11, although the identified
structures are much shorter, and thus smaller in $\Delta^{14}\text{C}$ (Fig. 3), than the hypothesized plateaus
would imply.

455

3.3/ Current ^{14}C sediment-based records do not have the resolution or precision in ^{14}C
measurement one might ideally desire – it is for this reason the community aims for the use of
tree-rings to construct the IntCal calibration curve. For example, the Lake Suigetsu record
(Bronk Ramsey et al. 2012) on which PT is based contains only 76 observations from 12-13.9
460 cal kyr BP with ^{14}C age uncertainties varying between 39 and 145 ^{14}C yrs (1σ). The Cariaco
record (Hughen et al. 2006) is one of the more highly-resolved collection of foraminifera yet
contains only 24 observations from 14-15.9 cal kyr BP with ^{14}C age measurement uncertainties
of around 40 ^{14}C yrs (1σ).

In light of such sparse sampling and measurement uncertainty, it is unclear how much
465 confidence one can have that identified ^{14}C -age plateaus, in the target Lake Suigetsu record and
the marine record one intends to tune, are genuine atmospheric phenomena and also that they
are correctly paired between the two records. One would need to be confident both that the
Lake Suigetsu record had identified all genuine atmospheric ^{14}C -age plateaus and further that
one can then pair each identified marine ^{14}C -age plateau correctly with its corresponding
470 atmospheric ^{14}C -age plateau, also taking into account that the marine ^{14}C -age plateau is offset
by an unknown surface marine reservoir age. Were one to fail to identify a genuine atmospheric
 ^{14}C -age plateau using the Lake Suigetsu record (e.g. were there to be 5 true atmospheric ^{14}C -
age plateaus but only 3 of these 5 plateaus are identifiable in the noisy Lake Suigetsu
observations and 3, potentially different plateaus, in the marine core to be tuned) then one
475 cannot presumably be sure to be matching the same ^{14}C -age plateaus between the records with
the consequential risk of severe misalignment of the marine core.

3.4/ In initially determining ^{14}C -age plateaus in the marine core, one does not have a



calendar time scale on which to provide a gradient (in terms of ^{14}C yr/cal yr). Without an ability
480 to work out the gradient per cal yr, identifying a ^{14}C -age plateau is considerably more
challenging. A natural option might be to use the depth scale within the core. This would be
equivalent to assuming a constant sedimentation rate. However, in then tying/matching
subsequent plateau to the atmospheric ^{14}C -age plateau this assumption of constant
485 sedimentation would be over-ridden and potentially significantly violated. In fact, in previous
work, the PT method appears to provide sedimentation rates which vary by up to a factor of 5
to 8 within a single core (e.g. cores PS2644 and MD08-3180 in Sarnthein et al. 2015; PS75/104-
1 in Küssner et al. 2018), considerably more, by orders of magnitude, in other cores from the
Nordic Seas (Sarnthein & Werner 2017), and even more in ad-hoc hiatuses mentioned above
490 in section 2.4. The question of how one identifies marine ^{14}C -age plateau in the context of a
changing and unknown sedimentation rate/calendar age scale – for which estimates only
become available after one has already been required to select plateaus and perform the tuning
– does not have a straightforward solution and is prone to confirmatory bias.

3.5/ The original PT method (Sarnthein et al. 2007, 2011) was based only on visual
495 inspection of the observed ^{14}C -ages vs depth to determine the ^{14}C -age plateaus (both the
duration of the plateaus and their constant ^{14}C ages including an unknown marine reservoir
age). In an attempt to reduce the subjectivity of eyeball evaluation, Sarnthein et al. (2015)
calculated the first derivative of a locally-fitted ^{14}C -age vs depth curve to identify the ^{14}C -age
plateaus (i.e. times when the slope drops to zero). This refinement goes in the right direction,
500 but the authors admit that there is room for subjectivity when choosing the level of smoothing
and the threshold for defining a plateau. In addition, their derivation technique apparently does
not consider explicitly the different analytical errors of the individual ^{14}C measurements that
are quite variable for Suigetsu ^{14}C data measured on small plant macrofossils of varying carbon
masses (Bronk Ramsey et al. 2012).

505 In any case, Sarnthein et al. (2015) chose to keep the visual inspection as their main
tool: “*we continued to base our calculations of reservoir ages, our tuned calendar ages of
plateau boundaries, and sedimentation rates on the boundary ages defined by visual
inspection.*”. In Sarnthein et al. (2020), it seems that eyeball inspection has been preferred
again: indeed Table 1 provides ^{14}C -age plateaus obtained “*by means of visual inspection*” in
510 the target records (Lake Suigetsu varved sediments and Hulu cave stalagmites).

3.6/ To assess objectively the ability to reliably identify and tune ^{14}C -age plateaus, in



the context of the noisy and sparse ^{14}C data currently available to us, we performed a simulation study. For this study, we aimed to investigate two aspects: firstly, can we reliably and robustly identify atmospheric ^{14}C -age plateaus in data that are of comparable density and precision to those from Lake Suigetsu; and secondly, having simulated paired ^{14}C age and depth data from a hypothetical marine core with comparable precision and density to the Cariaco Basin, can we use PT to accurately reconstruct the marine record's underlying calendar age scale?

Our simulated pseudo-Cariaco marine core is quite densely sampled compared with marine cores studied by Sarnthein et al. (2020). Moreover, we have simplified reality by setting a constant MRA for our simulated marine record. The additional complexities introduced to PT should MRAs change at any time other than plateau boundaries are not considered. Consequently, our simulation results should be considered a best-case scenario for the PT method.

Our study considers the period from 12-13.9 cal kyr BP and used the IntCal20 curve (Reimer et al. 2020) as our true atmospheric ^{14}C baseline. This is shown as a black line in Figure 5a-c. This period of IntCal20 is based upon ^{14}C determinations from highly-resolved tree-rings and so should reflect genuine atmospheric ^{14}C -age variation and plateaus. Even here though, exactly what would be considered to constitute a ^{14}C -age plateau, and how many are present, is ill-defined.

To this tree-ring based plateau baseline, we create a pseudo-Suigetsu atmospheric ^{14}C record by randomly sampling (fairly evenly-spaced) calendar ages between 12-13.9 cal kyr BP and adding noise comparable to that seen in the ^{14}C determinations of Lake Suigetsu. For this pseudo-atmospheric record, we assume the calendar ages of the ^{14}C determinations are known precisely, which aids plateau identification.

We also create a pseudo-Cariaco marine ^{14}C record by again sampling (fairly evenly-spaced) calendar ages and adding noise comparable to the ^{14}C determinations in the Cariaco Basin record (Hughen et al. 2006). To make this analogous to a genuine marine record PT, the calendar age information within the pseudo-marine record was then dropped and the ^{14}C measurements were assumed evenly-spaced in depth along the core. We sought to identify if we could then reconstruct this underlying calendar age information using PT.

To permit objectivity, we aimed to implement the automated ^{14}C -age plateau identification approach presented in Sarnthein et al. (2015). The description of their automated approach lacks precise detail to be completely reproducible, however, we hope that our method follows the principles sufficiently closely. Code is available on request.

We initially simulated three hypothetical cores recording atmospheric ^{14}C . These aimed



to represent data similar to Lake Suigetsu, both in terms of sampling density and ^{14}C age measurement uncertainties. There are 76 ^{14}C observations from Lake Suigetsu between 12 and 13.9 kcal BP. For each of our atmosphere-recording pseudo-cores, we sampled $N = 76$ observations as follows:

1. Simulate calendar ages θ_i :
 - Sample $U_k \sim \text{Unif}[12,13.9]$ for $k = 1, \dots, 2N$
 - Order sampled values to obtain $U_{(1)} < U_{(2)} < \dots < U_{(2N)}$
 - Set $\theta_i = U_{(2i)}$ for $i = 1, \dots, N$ (i.e. every 2nd ordered value)

This provides a set of random (but relatively-evenly sampled) calendar ages.

2. Simulate ^{14}C ages X_i , for $i = 1, \dots, N$ as $X_i \sim N(\mu(\theta_i), \sigma_i^2)$, where $\mu(\theta_i)$ is the mean of the IntCal20 curve at calendar age θ_i and σ_i^2 are the variances of the ^{14}C age measurements reported in the true Lake Suigetsu record.

To estimate the gradient at any given calendar age t , following as best we could the approach described in Sarnthein et al. (2015), we fitted a linear model to the nearest, in terms of calendar age, 60 observations weighted according to their reported uncertainties σ_i and a $N(0, 50^2 \text{ cal yr}^2)$ kernel centred on t – this gives a weighted moving window, where those observations more than 100-200 cal yr from t have little weight. In our idealized scenario, we assumed the calendar ages of the observations were known exactly for weighting and gradient estimation – in the genuine Lake Suigetsu record these calendar ages are themselves uncertain making gradient estimate somewhat harder.

Figures 5a-c show, for each of the three atmosphere-recording pseudo-cores, the simulated data and estimated gradient (with 95% intervals for the estimate obtained by the weighted linear model). Gradient estimates at the calendar age extremes should be treated with caution and so are not considered below. Fig. 5d shows the gradient estimates overlain with the suggested gradient threshold of $0.5 \text{ }^{14}\text{C yr/cal yr}$.

We observe that while the gradients obtained in each simulated core show some of the same main features, differences remain that are critical to PT. In particular, we see that the cut-off for identifying a plateau is key and selection is non-trivial if one wishes to maintain consistency between records. Additionally, the number of atmospheric ^{14}C -age plateaus seen in each record appears to vary. Within the green pseudo-core, we might identify 6 plateaus; whereas had we used the blue or red pseudo-core we might have identified anything from 3 to



580 5. Using different atmospheric records to initially identify ^{14}C -age plateaus could then lead to
different target matchings in marine records – not only might one be aiming to identify different
number of marine ^{14}C -age plateaus but also, if there are in fact more genuine atmospheric ^{14}C -
age plateaus than the atmospheric-recording core indicated, this could lead to erroneous
pairings between the atmospheric and marine cores. Furthermore, even with data this dense,
585 not all the dips in gradient estimate coincide – particularly notable around 13.4 cal kyr BP in
panel 5d.

3.7/ We also created two pseudo-marine ^{14}C records, aiming to mimic the relatively high
density and precision of the Cariaco Basin unvarved ^{14}C record (Hughen et al. 2006). These
590 simulated pseudo-marine cores are created similarly to the pseudo-atmospheric simulated
records above but, after creation, we remove the calendar age information that aids ^{14}C yr/cal
yr gradient calculation. Instead ^{14}C -age plateaus in the pseudo-marine must be identified using
only their ordering (or simulated depth) within the core – a considerably more challenging and
less robust task.

595 We create our simulated pseudo-marine cores to span 12-13.9 cal kyr BP, again using
IntCal20 as our true atmospheric ^{14}C baseline. We then compare them against our pseudo-
atmospheric cores to assess the ability to identify, and match, shared plateaus. For IntCal13, in
the 14-15.9 cal kyr time period, the Cariaco Basin unvarved ^{14}C record contained 24
observations (Hughen et al. 2006). Note that this 14-15.9 cal kyr period is used as representative
600 of sampling density since the Cariaco unvarved record does not extend to 12 cal kyr. For each
pseudo-marine core, mirroring the approach given in our pseudo-atmospheric simulated
records, we therefore simulated $N = 24$ random observations with underlying calendar ages
again sampled according to every 2nd ordered value of a uniform distribution to create relatively
equi-spaced ages ranging from 12-13.9 cal kyr BP. However, for these marine cores, we
605 selected ^{14}C age measurement uncertainties that matched those in the Cariaco Basin (1σ of
approximately 40 ^{14}C yr) and applied an adjustment of a constant MRA of 400 ^{14}C yrs. The
resultant simulations are shown in Fig 6 – with the simulated data shown in Fig. 6a. Since the
Cariaco Basin ^{14}C record is quite densely sampled compared to marine records studied by
Sarnthein et al. (2020), and we have applied a constant MRA, this set-up provides a best case
610 scenario for PT.

As discussed above, estimating the gradient (^{14}C yr/cal yr) and identifying ^{14}C -age
plateaus is made more complex here since, in a marine core, the calendar ages are unknown
before PT. One is therefore required to select a prior, pseudo-calendar, scale on which to



615 estimate a gradient and hence identify plateaus. We chose to estimate the gradient by assuming
our ^{14}C observations are equi-spaced in depth along the core as shown in Fig. 6b. Since, by
construction, our true calendar ages, θ_i , are relatively evenly-spaced this pseudo-calendar scale
should equate to a sedimentation rate which is not unrealistically variable. The inferred
sedimentation rate which would generate this equi-spacing in depth can be seen at the foot of
Fig. 6b. Such an equi-spacing can equivalently be interpreted as using the ordering-information
620 only to determine the gradient, i.e. the change we observe moving from one ^{14}C observation to
the next. This is a natural approach as it requires no a priori assumptions regarding the unknown
true calendar ages.

The same linear model approach as used for the pseudo-atmospheric cores was then
applied with weightings determined according to our even-depth observational spacing (i.e.
625 using the observational order only). We used the nearest 20 other marine ^{14}C observations and
a kernel on the depth scale analogous to the $N(0, 50^2 \text{ cal yr}^{-2})$ used for the pseudo-atmospheric
observations. This depth kernel was applied so that 50 cal yrs corresponded to 50/1900 of the
pseudo-marine core's depth (i.e. so the 1.9 kyr period between 12-13.9 cal kyr period covered
the full pseudo-marine core). The obtained gradient estimates for the cores are shown in Fig.
630 6b on this even-spacing (or observational order) basis.

We would select ^{14}C -age plateaus, and the observations belonging to them, based upon
Fig. 6b with its even-depth-spaced, pseudo-calendar timescale. For example, in pseudo-marine
core A we might identify an order-based plateau ending around the 5th observation (perhaps
covering the 1st to the 5th) since in this neighborhood the gradient on the pseudo-calendar scale
635 is low. We can infer where any such identified order-based ^{14}C -age plateaus correspond to on
the true calendar age timescale by transforming back from the ordered/even-depth spacing
using the underlying calendar ages of our observations. Fig. 6c shows the order-based gradient
estimates (and the observations in each simulated marine core) when plotted against the true
“unknown” calendar age timescale. In our example, the ^{14}C -age plateau identified between the
640 1st and 5th observation in pseudo-marine core A of Fig 6b corresponds to a ^{14}C -age plateau
covering the interval 12-12.5 cal kyr BP.

In Fig. 6d, we overlay the order-based marine-core gradients, after they have been
transformed back to their true underlying timescales, against the gradient obtained from our
first simulated pseudo-atmospheric record. For PT tuning to provide reliable MRA estimates,
645 the dips/plateaus in the pseudo-marine core and the pseudo-atmospheric core should align in
Fig. 6d. This does not occur. The large amount of noise in the marine records, their sparsity,
and their unknown true time scale mean that one would potentially identify very different ^{14}C -



age plateaus in the different simulated marine records. Furthermore, the marine ^{14}C -age plateaus may not correspond to the ^{14}C -age plateaus in the atmospheric record. Consequently, one would miss-estimate MRA changes and obtain incorrect timescales for the marine cores.

While simple, this simulation study illustrates some of the potential difficulties of identifying plateaus in the presence of observational noise. Were the simulated data to have much higher precision and be sampled much more densely, we would expect the ^{14}C -age plateaus to align more consistently. Such a preliminary study with an exact and reproducible approach is needed to assess the robustness of the method. The fundamental questions of how to remove the potentially confounding effects of MRA changes and other potential geoscientific factors in identifying ^{14}C -age plateaus will however still remain.

3.8/ Finally, implicit in the Sarnthein et al. (2020) paper is a suggestion that using Lake Suigetsu alone provides a more precise reconstruction of atmospheric ^{14}C levels from 55 – 13.9 cal kyr BP than the IntCal20 synthesis (Reimer et al. 2020). Specifically, that by combining ^{14}C records from a diverse range of archives, the IntCal curves lose genuine atmospheric structure that can be extracted from Suigetsu. This perspective is suggested by Sarnthein et al. (2020) through an argument that the IntCal20 curve has lesser variation, and fewer wiggles, from 55 – 13.9 cal kyr BP, where it is based upon a range of archives, than from 13.9-0 cal kyr BP, where it is based upon highly resolved tree-ring determinations.

Indeed, Reimer et al. (2020) recognize the limitations of the current archives on which they base the IntCal20 curves and the ideal for a truly atmospheric ^{14}C record extending back to 55,000 cal BP, that also provides sufficient detail to reliably and precisely reconstruct the high-frequency component of the ^{14}C signal. However, this characterization of IntCal20, as overly smooth and hence unreliable from 55 – 13.9 cal kyr BP, is to misunderstand what the IntCal curve represents.

The values published as the IntCal curves aim to provide pointwise summaries of the ^{14}C age, in terms of the mean and uncertainty, at any chosen calendar age. This is not the same as trying to represent the level of ^{14}C variation from one year to the next. Critically, a smooth pointwise mean does not necessarily imply no variation in atmospheric ^{14}C levels. More likely, it represents that we do not yet know when, and with what magnitude, any such ^{14}C variations occur.

Construction of the IntCal20 curve uses Bayesian splines (Heaton al. 2020b). The outputs of this Bayesian approach are a large set of posterior curve realisations that aim to find a trade-off between passing near the observed ^{14}C determinations on which the curve is based,



while not being so variable as to overfit and introduce spurious features. The pointwise summary is then based upon averaging over 2,500 of these curve realisations.

685 The IntCal approach does, in fact, assume there are similar levels of short-term atmospheric variability from 55 – 13.9 cal kyr as in the tree-ring based section from 13.9 – 0 cal kyr BP. This can be seen by looking at 5 individual posterior realisations, randomly selected from the 2500 used to create the final IntCal20 pointwise summary, shown in Figure 7. All of these individual realisations exhibit significant short term ^{14}C variability, although none on the scale of the hypothesized Sarnthein et al. (2020) plateaus as they must still agree with the pointwise IntCal uncertainties (shown at 2σ as the dotted purple envelope). However, as we do not yet have sufficiently detailed ^{14}C measurements, the precise timing and magnitude of the fluctuations in the realisations is unknown. Consequently, when averaged to provide the pointwise estimates, these realisations provide an IntCal pointwise mean (shown as solid purple) that is smoother than any individual realisation.

690



695 **References:**

- Adolphi, F. and Muscheler, R. Synchronizing the Greenland ice core and radiocarbon timescales over the Holocene-Bayesian wiggle-matching of cosmogenic radionuclide records. *Climate of the Past*, 12(1), 15-30. doi:10.5194/cp-12-15-2016, 2016.
- 700 Adolphi, F., Muscheler, R., Friedrich, M., Gütler, D., Wacker, L., Talamo, S. and Kromer, B. Radiocarbon calibration uncertainties during the last deglaciation: Insights from new floating tree-ring chronologies. *Quaternary Science Reviews*, 170, 98-108, doi:10.1016/j.quascirev.2017.06.026, 2017.
- 705 Adolphi, F., Bronk Ramsey, C., Erhardt, T., Lawrence Edwards, R., Cheng, H., Turney, C.S.M., Cooper, A., Svensson, A., Rasmussen, S.O., Fischer, H. and Muscheler, R. Connecting the Greenland ice-core and U/Th timescales via cosmogenic radionuclides: Testing the synchronicity of Dansgaard-Oeschger events. *Climate of the Past*, 14, 1755-1781, doi:10.5194/cp-2018-85, 2018.
- 710 Andrews, A., Siciliano, D., Potts, D., DeMartini, E., & Covarrubias, S. Bomb Radiocarbon and the Hawaiian Archipelago: Coral, Otoliths, and Seawater. *Radiocarbon*, 58(3), 531-548. doi:10.1017/RDC.2016.32, 2016.
- 715 Ausin, B., Haghpor, N., Wacker, L., Voelker, A. H. L., Hodell, D., Magill, C., Looser N., Bernasconi S.M., Eglinton T.I. Radiocarbon age offsets between two surface dwelling planktonic foraminifera species during abrupt climate events in the SW Iberian margin. *Paleoceanography and Paleoclimatology*, 34, 63-78, doi: 10.1029/2018PA003490, 2019
- 720 Balmer, S., Sarnthein, M., Mudelsee, M., and Grootes, P. M.: Refined modeling and ¹⁴C plateau tuning reveal consistent patterns of glacial and deglacial ¹⁴C reservoir ages of surface waters in low-latitude Atlantic. *Paleoceanography*, 31. doi:10.1002/2016PA002953, 2016.
- 725 Balmer, S. and Sarnthein, M.: Glacial-to deglacial changes in North Atlantic meltwater advection and deep-water formation – Centennial-to-millennial-scale ¹⁴C records from the Azores Plateau. *Geochimica et Cosmochimica Acta*, 236, 399-415, doi:10.1016/j.gca.2018.03.001, 2018.
- 730 Bard, E. Correction of accelerator mass spectrometry ¹⁴C ages measured on planktonic foraminifera: Paleooceanographic implications. *Paleoceanography*, 3, 635-645. doi:10.1029/PA003i006p00635, 1988.
- 735 Bard, E. Geochemical and geophysical implications of the radiocarbon calibration. *Geochimica et Cosmochimica Acta*, 62, 2025-2038. doi:10.1016/S0016-7037(98)00130-6, 1998.
- Bard, E., Arnold, M., Duprat, J., Moyes, J. and Duplessy, J.C. Reconstruction of the last deglaciation: deconvolved records of $\delta^{18}\text{O}$ profiles, micropaleontological variations and accelerator mass spectrometric ¹⁴C dating. *Climate Dynamics*, 1, 101-112. doi:10.1007/BF01054479, 1987.
- 740 Bard, E., Arnold, M., Mangerud, M., Paterne, M., Labeyrie, L., Duprat, J., Mélières, M.A., Sonstegaard, E., Duplessy, J.C. The North Atlantic atmosphere-sea surface ¹⁴C gradient during the Younger Dryas climatic event. *Earth and Planetary Science Letters* 126, 275-287. doi:



- 745 10.1016/0012-821X(94)90112-0, 1994.
- Bard, E., Raisbeck, G., Yiou, F., Jouzel, J. Solar modulation of cosmogenic nuclide production over the last millennium: comparison between ^{14}C and ^{10}Be records. *Earth and Planetary Science Letters* 150, 453-462. doi: 10.1016/S0012-821X(97)00082-4, 1997.
- 750 Beer, J., Siegenthaler U., Bonani G., Finkel R.C., Oeschger H., Suter M., Wölfli W. Information on past solar activity and geomagnetism from ^{10}Be in the Camp Century ice core, *Nature* 331, 675-679. doi:10.1038/331675a0, 1988.
- 755 Broecker, W., Mix A.C., Andree M., Oeschger H., Radiocarbon measurements on coexisting benthic and planktic foraminifera shells: potential for reconstructing ocean ventilation times over the past 20 000 years, *Nuclear Instruments and Methods B*, 5 (2), 331-339, doi: 10.1016/0168-583X(84)90538-X, 1984.
- 760 Bronk Ramsey, C., van der Plicht, J., Weninger, B. "Wiggle matching" radiocarbon dates. *Radiocarbon* 43(2), 381-389, doi:10.1017/S0033822200038248, 2001.
- Bronk Ramsey, C., Staff, R.A., Bryant, C.L., Brock, F., Kitagawa, H., van der Plicht, J., Scholaut, G., Marshall, M.H., Brauer, A., Lamb, H.F., Payne, R.L., Tarasov, P.E., Haraguchi, T., Gotanda, K., Yonenobu, H., Yokoyama, Y., Tada, R., Nakagawa, T., A Complete terrestrial radiocarbon record for 11.2 to 52.8 kyr BP. *Science* 338:370-374, 2012.
- 765 Bronk Ramsey, C., Heaton, T.J., Scholaut, G., Staff, R.A., Bryant, C.L., Brauer, A., Lamb, H.F., Marshall, M.H., Nakagawa, T. Reanalysis of the atmospheric radiocarbon calibration record from Lake Suigetsu, Japan. *Radiocarbon* 62, 989-999, doi: 10.1017/RDC.2020.18, 2020.
- Butzin, M., Prange, M. and Lohmann, G. Radiocarbon simulations for the glacial ocean: the effects of wind stress, Southern Ocean sea ice and Heinrich events. *Earth and Planetary Science Letters*, 235, 45-61. doi:10.1016/j.epsl.2005.03.003, 2005.
- 775 Capano, M., Miramont, C., Shindo, L., Guibal, F., Marschal, C., Kromer, B., Tuna, T., Bard, E. Onset of the Younger Dryas recorded with ^{14}C at annual resolution in French subfossil trees. *Radiocarbon*, doi:10.1017/RDC.2019.116, 2020.
- 780 Cheng, H., Edwards, R.L., Southon, J., Matsumoto, K., Feinberg, J.M., Sinha, A., Zhou, W., Li, H., Li, X. and Xu, Y. Atmospheric $^{14}\text{C}/^{12}\text{C}$ changes during the last glacial period from Hulu Cave. *Science*, 362(6420), 1293-1297, 2018.
- 785 Costa, K., McManus, J. and Anderson, R. Radiocarbon and Stable Isotope Evidence for Changes in Sediment Mixing in the North Pacific over the Past 30 kyr. *Radiocarbon*, 60(1), 113-135. doi:10.1017/RDC.2017.91, 2018.
- 790 de la Fuente, M., Skinner, L., Calvo, E., Pelejero, C., Cacho, I. Increased reservoir ages and poorly ventilated deep waters inferred in the glacial Eastern Equatorial Pacific. *Nat. Commun.* 6:7420 doi: 10.1038/ncomms8420, 2015.
- Delaygue, G., Stocker, T.F., Joos, F. and Plattner, G.-K. Simulation of atmospheric radiocarbon during abrupt oceanic circulation changes: trying to reconcile models and reconstructions.



- 795 *Quaternary Science Reviews*, 22, 1647-1658. doi:10.1016/S0277-3791(03)00171-9, 2003.
- Delaygue, G., Bard, E. An Antarctic view of beryllium-10 and solar activity for the past millennium. *Climate Dynamics* 36, 2201-2218, DOI:10.1007/s00382-010-0795-1, 2011.
- 800 Franke, J., Paul, A. and Schulz, M. Modeling variations of marine reservoir ages during the last 45 000 years. *Climate of the Past*, 4, 125-136. doi:10.5194/cp-4-125-2008, 2008.
- Fournier, A., Gallet Y., Usoskin I., Livermore P.W., and Kovaltsov G.A., The impact of geomagnetic spikes on the production rates of cosmogenic ^{14}C and ^{10}Be in the Earth's atmosphere, *Geophys. Res. Lett.*, 42, 2759–2766, doi:10.1002/2015GL063461, 2015.
- 805
- Goslar, T., Arnold, M., Bard, E., Kuc, T., Pazdur, M.F., Ralska-Jasiewiczowa, M., Rozanski, K., Tisnerat, N., Walanus, A., Wicik, B. and Wieckowski, K. High concentration of atmospheric ^{14}C during the Younger Dryas cold episode. *Nature*, 377, 414-417. doi:10.1038/377414a0, 1995.
- 810
- Grottoli A.G., Eakin C.M., A review of modern coral $\delta^{18}\text{O}$ and $\Delta^{14}\text{C}$ proxy records, *Earth-Science Reviews*, 81, (1–2), 67-91, doi:10.1016/j.earscirev.2006.10.001, 2007.
- 815 Heaton, T.J., Köhler, P., Butzin, M., Bard, E., Reimer, R.W., Austin, W.E.N., Bronk Ramsey, C., Grootes, P.M., Hughen, K.A., Kromer, B., Reimer, P.J., Adkins, J.F., Burke, A., Cook, M.S., Olsen, J., Skinner, L.C.. Marine20 - the marine radiocarbon age calibration curve (0-55,000 cal BP). *Radiocarbon* 62, 821-863, DOI: 10.1017/RDC.2020.68, 2020a.
- 820 Heaton, T.J., Blaauw, M., Blackwell, P.G., Bronk Ramsey, C., Reimer, P.J., Scott, E.M. The IntCal20 approach to radiocarbon calibration curve construction: a new methodology using Bayesian splines and errors-in-variables. *Radiocarbon* 62, 821-863, doi: 10.1017/RDC.2020.46 2020b.
- 825 Hughen, K.A., Overpeck, J.T., Lehman, S.J., Kashgarian, M., Southon, J., Peterson, L.C., Alley, R., and Sigman, D.M. Deglacial changes in ocean circulation from an extended radiocarbon calibration. *Nature*, 391, 65–68. doi:10.1038/34150, 1998.
- Hughen, K.A., Southon, J.A., Lehman, S.J., Bertrand, C.J.H., Turnbull, J. Marine-Derived ^{14}C Calibration and activity record for the past 50,000 years updated from the Cariaco Basin, *Quaternary Science Reviews* 25: 3216-3227, 2006.
- 830
- Imbrie, J., Kipp, N.G., A new micropaleontological method for quantitative paleoclimatology: application to a late Pleistocene Caribbean core. In: Turekian, K.K. (Ed.), Late Cenozoic Glacial Ages. Yale Univ. Press, New Haven, CN, 71-182, 1971.
- 835
- Kucera M., Weinelt M., Kiefer T., Pflaumann U., Hayes A., Weinelt M., Chen M.-T., Mix A.C., Barrows T.T., Cortijo E., Duprat J., Juggins S., Waelbroeck C., Reconstruction of sea-surface temperatures from assemblages of planktonic foraminifera: multi-technique approach based on geographically constrained calibration data sets and its application to glacial Atlantic and Pacific Oceans, *Quaternary Science Reviews*, 24 (7-9), 951-998, doi:10.1016/j.quascirev.2004.07.014, 2005.
- 840
- Küssner, K., Sarnthein, M., Lamy, F., and Tiedemann, R.: High-resolution radiocarbon based



- 845 age records trace episodes of Zoophycos burrowing, *Marine Geology*, 403, 48-56, doi:10.1016/j.margeo.2018.04.01, 2018.
- Levin, I., & Heshaimer, V. Radiocarbon – A Unique Tracer of Global Carbon Cycle Dynamics. *Radiocarbon*, 42(1), 69-80. doi:10.1017/S0033822200053066, 2000.
- 850 Marchal, O., Stocker, T.F., Muscheler, R. Atmospheric radiocarbon during the Younger Dryas: production, ventilation, or both? *Earth and Planetary Science Letters* 185, 383–395, doi: 10.1016/S0277-3791(03)00171-9, 2001.
- 855 Mekhaldi, F., Muscheler, R., Adolphi, F., Aldahan, A., Beer, J., McConnell, J.R., Possnert, G., Sigl, M., Svensson, A., Synal, H.A., Welten, K.C., Woodruff, E.T., Multiradionuclide evidence for the solar origin of the cosmic-ray events of AD 774/5 and 993/4. *Nat. Commun.* 6, 8611, doi: 10.1038/ncomms9611, 2015.
- 860 Miyake, F., Nagaya, K., Masuda, K., Nakamura, T., A signature of cosmic-ray increase in AD 774–775 from tree rings in Japan. *Nature* 486, 240–242, doi: 10.1038/nature11123, 2012.
- Muscheler, R., Joos, F., Beer, J., Muller, S.A., Vonmoos, M. and Snowball, I. Solar activity during the last 1000 yr inferred from radionuclide records. *Quaternary Science Reviews*, 26(1-2), 82-97. doi:10.1016/J.Quascirev.2006.07.012, 2007.
- 865 Oeschger, H., Welten, M., Eicher, U., Möll, M., Riesen, T., Siegenthaler, U., and Wegmüller, S. ¹⁴C and other parameters during the Younger Dryas cold phase. *Radiocarbon* 22, 299–310. doi:10.1017/S0033822200009590, 1980.
- 870 Reimer, P.J., Baillie, M.G.L., Bard, E., Bayliss, A., Beck, J.W., Blackwell, P.G., Bronk Ramsey, C., Buck, C.E., Burr, G.S., Edwards, R.L., Friedrich, M., Grootes, P.M., Guilderson, T.P., Hajdas, I., Heaton, T.J., Hogg, A.G., Hughen, K.A., Kaiser, K.F., Kromer, B., McCormac, F.G., Manning, S.W., Reimer, R.W., Richards, D.A., Southon, J.R., Talamo, S., Turney, C.S.M., van der Plicht, J., Weyhenmeyer, C.E. IntCal09 and Marine09 radiocarbon age calibration curves, 0–50,000 years cal BP. *Radiocarbon* 51 (4), 1111–1150, doi: 10.1017/S0033822200034202, 2009.
- 875 Reimer, P.J., Bard, E., Bayliss, A., Beck, J.W., Blackwell, P.G., Bronk Ramsey, C., Buck, C.E., Cheng, H., Edwards, R.L., Friedrich, M., Grootes, P.M., Guilderson, T.P., Haflidason, H., Hajdas, I., Hatté, C., Heaton, T.J., Hoffmann, D.L., Hogg, A.G., Hughen, K.A., Kaiser, K.F., Kromer, B., Manning, S.W., Niu, M., Reimer, R.W., Richards, D.A., Scott, E.M., Southon, J.R., Staff, R.A., Turney, C.S.M. and van der Plicht, J. IntCal13 and Marine13 Radiocarbon Age Calibration Curves 0-50,000 Years cal BP. *Radiocarbon*, 55(4), 1869-1887. doi:10.2458/azu_js_rc.55.16947, 2013.
- 885 Reimer P.J., Austin W.E.N., Bard E., Bayliss A., Blackwell P.G., Bronk Ramsey C., Butzin M., Cheng H., Edwards R.L., Friedrich M., Grootes P.M., Guilderson T.P., Hajdas I., Heaton T.J., Hogg A.G., Hughen K.A., Kromer B., Manning S.W., Muscheler R., Palmer J.G., Pearson C., van der Plicht H., Reimer R.W., Richards D., Scott E.M., Southon J.R., Turney C.S.M., Wacker L., Adolphi F., Büntgen U., Capano M., Fahrni S., Fogtmann-Schulz A., Friedrich R., Kudsk S., Miyake F., Olsen J., Reinig F., Minoru Sakamoto M., Sookdeo A., Talamo S. The IntCal20 Northern Hemisphere radiocarbon calibration curve (0-55 kcal BP). *Radiocarbon* 62, 725-757, doi: 10.1017/RDC.2020.41, 2020.



- 895 Ritz, S.P., Stocker, T.F. and Müller, S.A. Modeling the effect of abrupt ocean circulation change on marine reservoir age. *Earth and Planetary Science Letters*, 268, 202-211, doi:10.1016/j.epsl.2008.01.024, 2008.
- 900 Sarnthein, M., Grootes, P.M., Kennett, J.P., Nadeau, M.J. ¹⁴C Reservoir ages show deglacial changes in ocean currents, in: *Ocean Circulation: Mechanisms and Impacts*, Geophysical Monograph Series 173, edited by: Schmittner, A., Chiang, J., and Hemming, S., American Geophysical Union, Washington, DC, 175-197, doi: 10.1029/173GM0X, 2007.
- 905 Sarnthein, M., Grootes, P.M., Holbourn, A., Kuhnt, W., and Kühn, H.: Tropical warming in the Timor Sea led deglacial Antarctic warming and almost coeval atmospheric CO₂ rise by >500 yr, *Earth Planetary Science Letters*, 302, 337-348, doi:10.1016/j.epsl.2010.12.021, 2011.
- 910 Sarnthein, M., Schneider, B., and Grootes, P.M.: Peak glacial ¹⁴C ventilation ages suggest major draw-down of carbon into the abyssal ocean, *Climate of the Past*, 9 (1), 925-965, doi:10.5194/cp-9-2595-2013, 2013.
- 915 Sarnthein, M., Balmer, S., Grootes, P.M., and Mudelsee, M.: Planktic and benthic ¹⁴C reservoir ages for three ocean basins, calibrated by a suite of ¹⁴C plateaus in the glacial-to-deglacial Suigetsu atmospheric ¹⁴C record, *Radiocarbon*, 57, 129-151, doi:10.2458/azu_rc.57.17916, 2015.
- 920 Sarnthein, M. and Werner, K.: Early Holocene planktic foraminifers record species specific ¹⁴C reservoir ages in Arctic Gateway, *Marine Micropaleontology*, 135, 45-55, doi:10.1016/j.marmicro.2017.07.002, 2017.
- 925 Sarnthein, M., Küssner, K., Grootes, P.M., Ausin, B., Eglinton, T., Muglia, J., Muscheler, R., Scholaut, G. Plateaus and jumps in the atmospheric radiocarbon record – Potential origin and value as global age markers for glacial-to-deglacial paleoceanography, a synthesis. *Climate of the Past*, 16, 2547–2571, doi: 10.5194/cp-16-2547-2020, 2020
- 930 Singarayer, J.S., Richards, D.A., Ridgwell, A., Valdes, P.J., Austin, W.E.N. and Beck, J.W. An oceanic origin for the increase of atmospheric radiocarbon during the Younger Dryas. *Geophysical Research Letters*, 35, L14707. doi:10.1029/2008GL034074, 2008.
- 935 Stocker, T.F. and Wright, D.G. Rapid changes in ocean circulation and atmospheric radiocarbon. *Paleoceanography*, 11, 773-795. doi:10.1029/96PA02640, 1996.
- 935 Stocker, T.F. and Wright, D.G. The effect of a succession of ocean ventilation changes on ¹⁴C. *Radiocarbon*, 40(1), 359-366. doi:10.1017/S0033822200018233, 1998
- 940 Svetlik, I., Jull, A., Molnár, M., Povinec, P., Kolář, T., Demján, P., Pachnerova Brabcova K, Brychova V, Dreslerová D, Rybníček M, Simek, P. The Best possible time resolution: How precise could a radiocarbon dating method be? *Radiocarbon*, 61(6), 1729-1740. doi:10.1017/RDC.2019.134, 2019
- Umling, N. E. and Thunell R. C. Synchronous deglacial thermocline and deep-water ventilation in the eastern equatorial Pacific. *Nat. Commun.* 8, 14203 doi: 10.1038/ncomms14203 (2017).



945 **Figure captions:**

Figure 1: Blue dots show the Lake Suigetsu ^{14}C data with their 1σ analytical uncertainties in both radiocarbon and calendar age (Bronk Ramsey et al. 2020). The thin red line shows the pointwise posterior mean of the radiocarbon calibration curve based only on the Suigetsu data
950 using the same Bayesian statistical method used for IntCal20 (Heaton et al., 2020b, Reimer et al. 2020). The shaded interval represents the 95% posterior predictive probability interval. Superimposed thick green lines indicate the 15 atmospheric plateaus with their numbering listed in Table 1 of Sarnthein et al. (2020).

955 **Figure 2:** The thin purple line shows the pointwise posterior mean of the IntCal20 curve with its shaded interval representing the 95% posterior predictive probability interval (Reimer et al. 2020, Heaton et al., 2020b). Superimposed thick green lines indicate the 15 atmospheric plateaus with their numbering listed in Table 1 of Sarnthein et al. (2020).

960 **Figure 3:** The two panels represent the same data shown in Figs. 1 and 2, but converted in $\Delta^{14}\text{C}$ unit in ‰. Short (or zero) gaps between plateaus are transformed into abrupt rises. Age plateaus correspond to the second parts of these atmospheric $\Delta^{14}\text{C}$ wiggles, during which the $\Delta^{14}\text{C}$ decrease compensates the radioactive decay.

965 **Figure 4: 4a/** Amplitude ratio of $\Delta^{14}\text{C}$ wiggles in the atmosphere and the surface ocean created by sinusoidal changes of the ^{14}C production as an input to the 12-box model shown in the upper insert (Bard et al. 1997). This normalized attenuation factor is plotted versus the signal period of production variations (in log scale). The factor would be equal to 1 if atmospheric and oceanic amplitudes were the same. The light blue dashed curve shows the calculation results
970 for the Indo-Pacific surface box, while the dark blue dotted line stands for the Southern Ocean surface box. These two boxes differ by their surface ^{14}C reservoir age at steady state (320 and 890 yr for the Indo-Pacific and Southern Ocean surface boxes, respectively). The vertical dash-dot black line underlines the 500-yr period wiggle used to construct Fig.4b. The inset graph shows the geometry of the model by Bard et al. (1997) with numbers on boxes indicating their
975 steady-state $\Delta^{14}\text{C}$ (‰), numbers in parenthesis stand for halving the thermohaline circulation.

4b: ^{14}C age versus calendar age plot computed for sinusoidal ^{14}C production wiggles with a period of 500 years and an amplitude change of $\pm 15\%$ around the mean value (in order to produce oscillations around the 1:1 line, ^{14}C ages are calculated with the true half-life of



5730 yr). The red solid curve shows the evolution for the tropospheric box, exhibiting ^{14}C plateaus (marked with black arrows) when the slope of the relationship goes down to zero. The age plateau corresponds to the second part of the atmospheric $\Delta^{14}\text{C}$ wiggle, during which the $\Delta^{14}\text{C}$ decrease compensates the radioactive decay. The light blue dashed curve shows the calculation results for the Indo-Pacific surface box, while the dark blue dotted line stands for the Southern Ocean surface box. The blue curves are offset with respect to the atmospheric curve by their respective marine reservoir ages. In both cases, the slope of the relationship does not decrease to zero, implying the absence of true ^{14}C age plateaus in the surface ocean.

Figure 5: Simulation study to identify the ability of a Suigetsu-style record to reliably identify atmospheric ^{14}C -age plateaus. In Figs. 5a-c we present three simulated atmospheric records generated by sampling, subject to noise, from the high-precision tree-ring-based section of IntCal20 between 12-13.9 cal kyr BP (shown as a black line) with a sampling density matching that of Lake Suigetsu. The level of noise added to create these simulated ^{14}C observations (blue, red and green dots) was also of an equivalent level to that present in the Lake Suigetsu ^{14}C . For each simulated set of observations, we present an estimate of the local gradient (shown as blue, red and green curves with their 95% confidence intervals) according to a locally-weighted linear model as proposed by Sarnthein et al. (2015). In panel 5d we overlay the gradient estimates to assess consistency (or lack of) between the three simulated cores in terms of the number and location of ^{14}C -age plateaus one might identify.

Figure 6: Simulation study to identify the ability to identify ^{14}C -age plateaus in marine records for which calendar age scales are not initially known. In panel 6a we simulate two marine records between 12-13.9 cal kyr BP, again using the IntCal20 tree-ring-based record as the ground truth. These simulated marine cores are based upon the sampling density of the Cariaco Basin unvarved record, with a similar level of observational ^{14}C noise, and have been created with a constant MRA of 400 ^{14}C yrs. To identify plateaus, we first estimate the gradient on the basis of an unknown calendar age scale. We create a pseudo-calendar age scale by rescaling the observations so they are equi-spaced along the cores. Estimates of gradients, and implied relative sedimentation rates, on such an equi-spaced pseudo-timescale are provided in Fig. 6b. Scaling back to the true, underlying calendar age timescale, Fig. 6c indicates where, in terms of the actual calendar age scale, one might classify plateaus. These are overlain against the first of our pseudo-atmospheric simulated records of Fig 5 to assess synchronicity.



Figure 7: Plot of five individual spline realisations randomly selected from the Bayesian posterior of the Markov Chain Monte Carlo approach used to create IntCal20. The published
1015 IntCal20 consists of pointwise means (shown as purple solid line) and 95% pointwise predictive intervals (purple dotted line) which are obtained by averaging over 2500 of these individual curve realisations (Heaton et al. 2020). Superimposed thick green lines indicate the 15 atmospheric plateaus with their numbering listed in Table 1 of Sarnthein et al. (2020).

1020

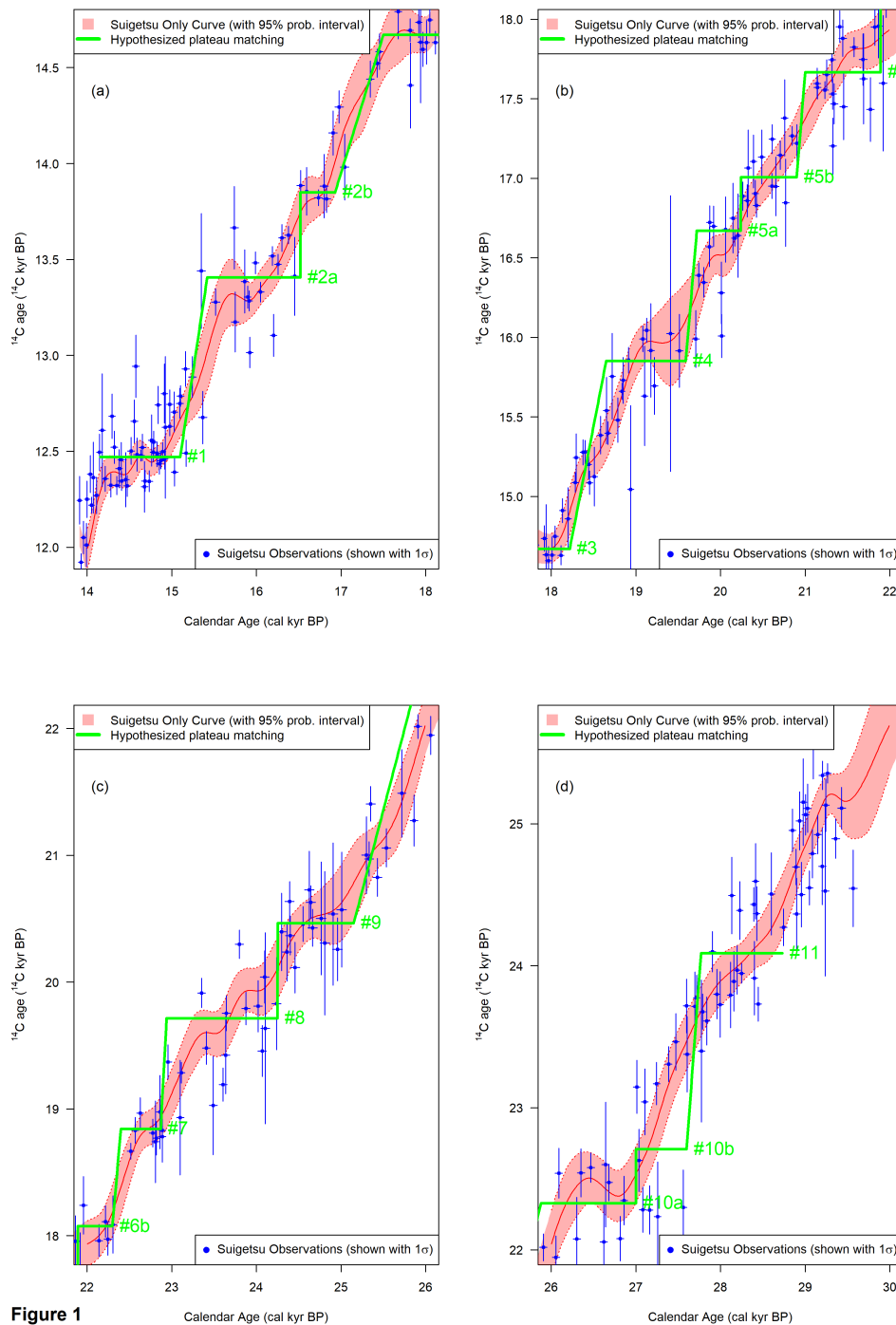


Figure 1

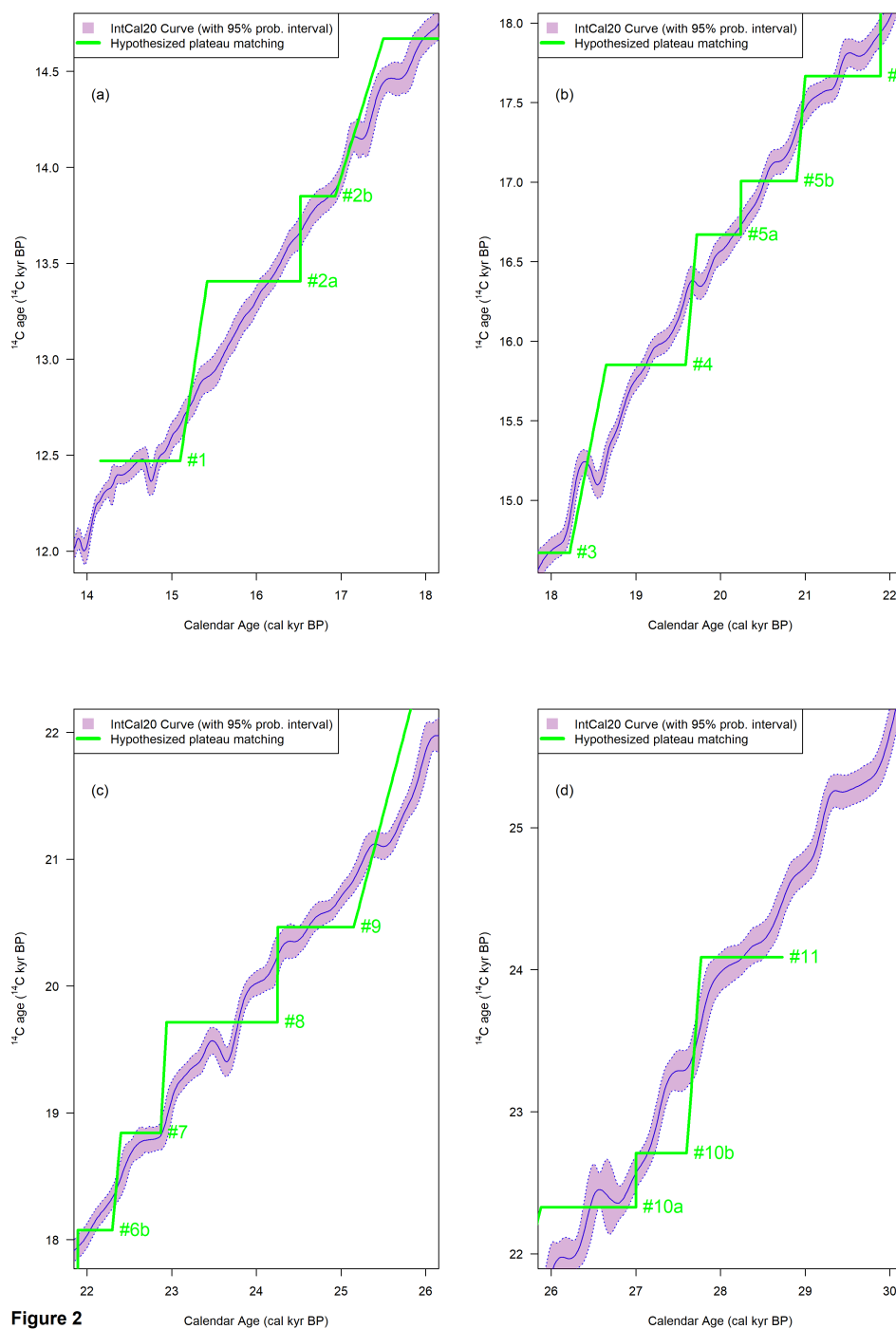
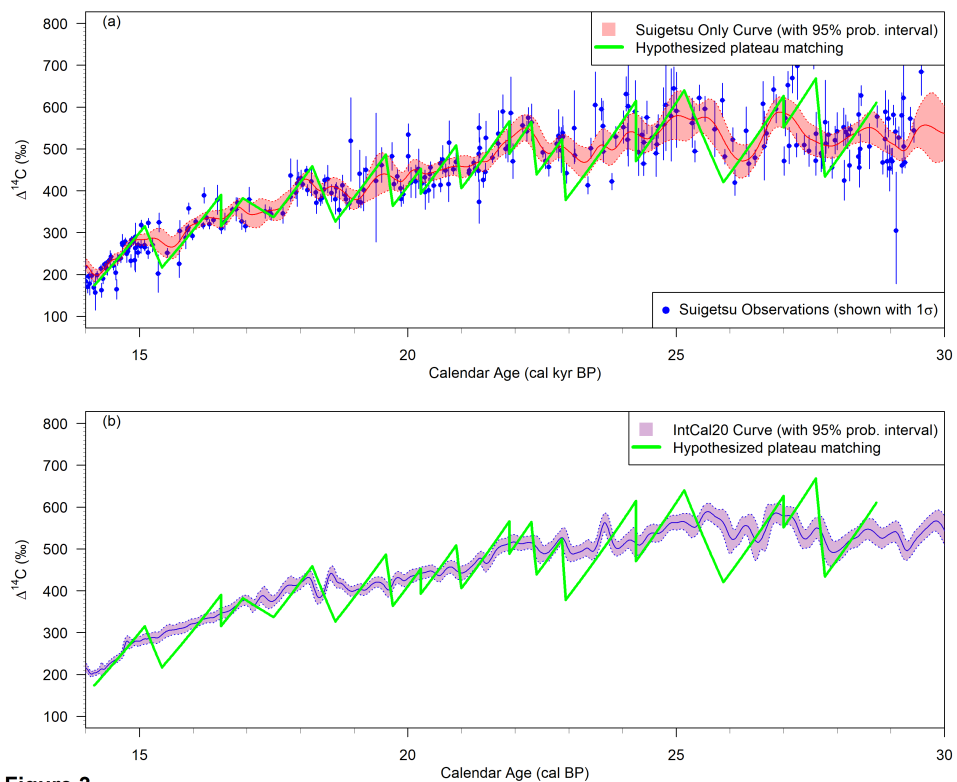


Figure 2



1025 **Figure 3**

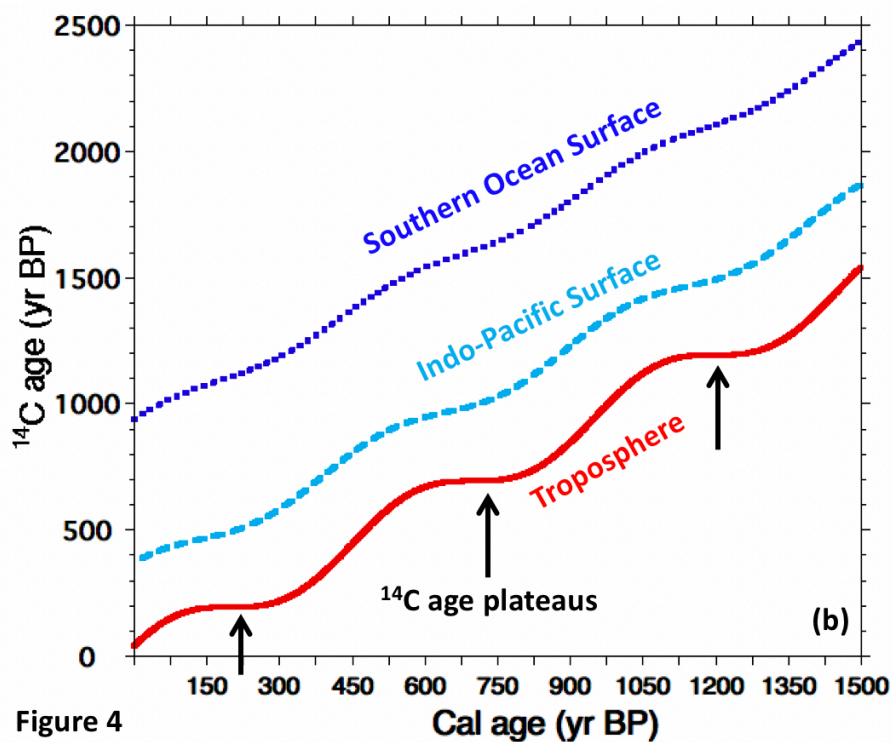
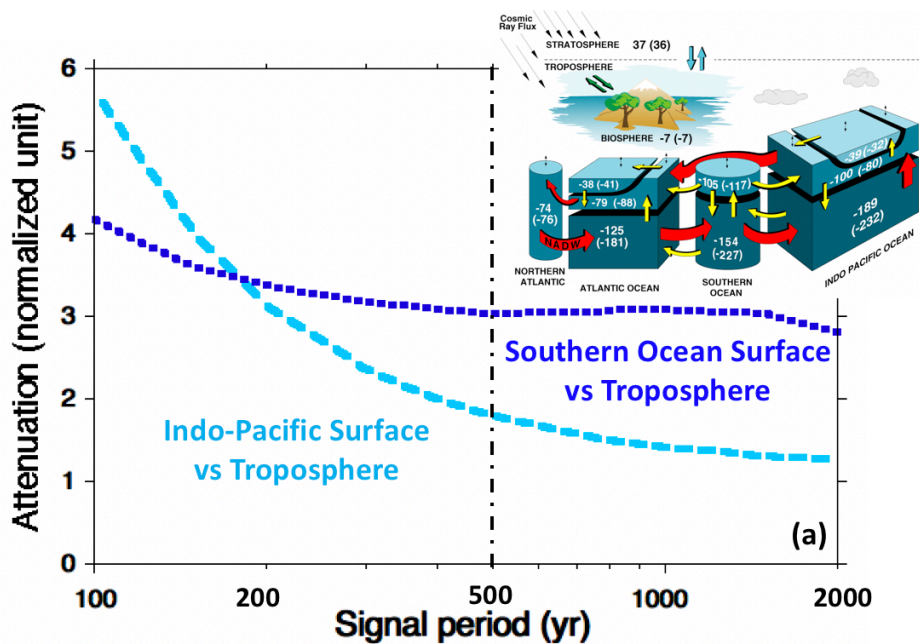


Figure 4

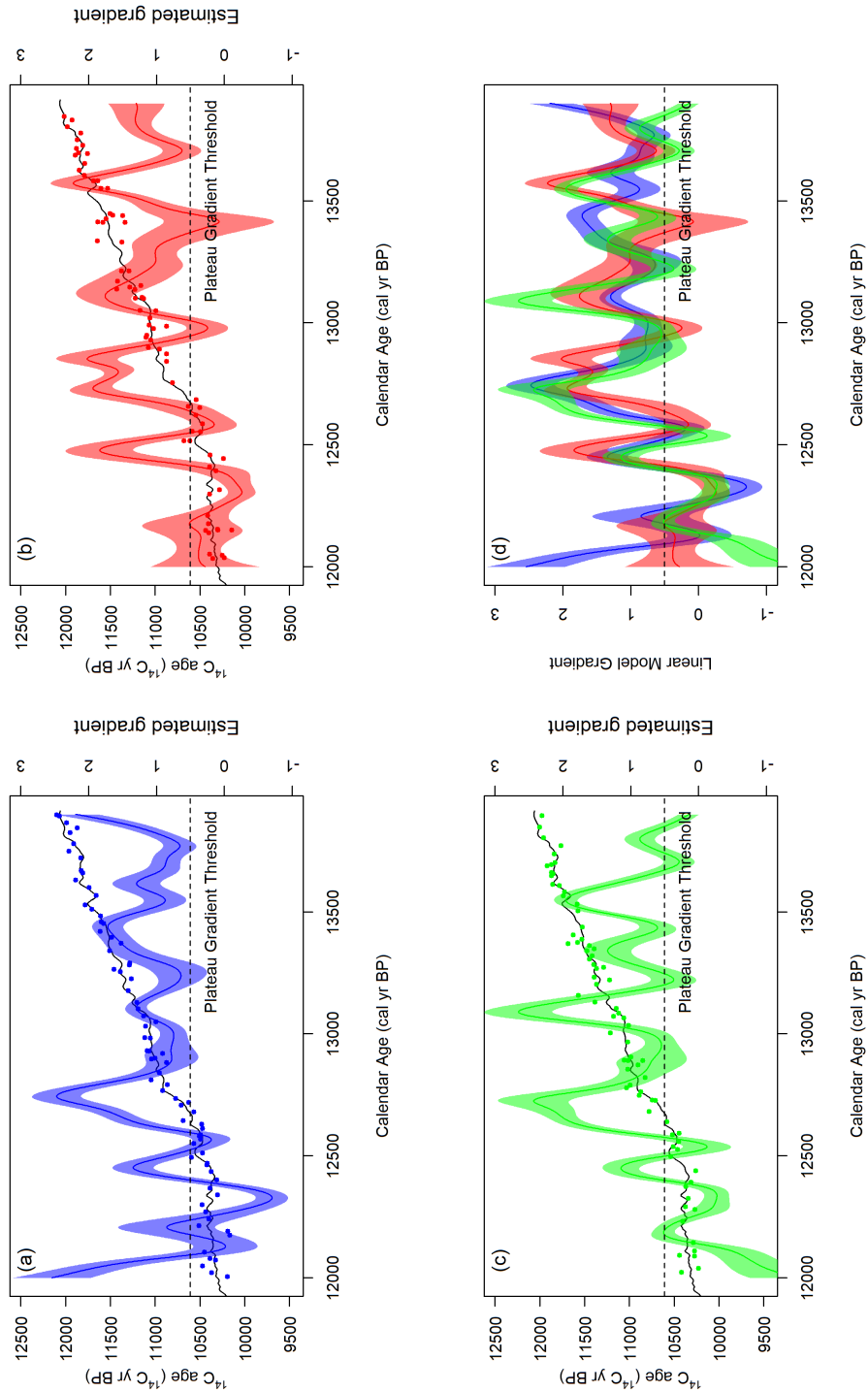


Figure 5

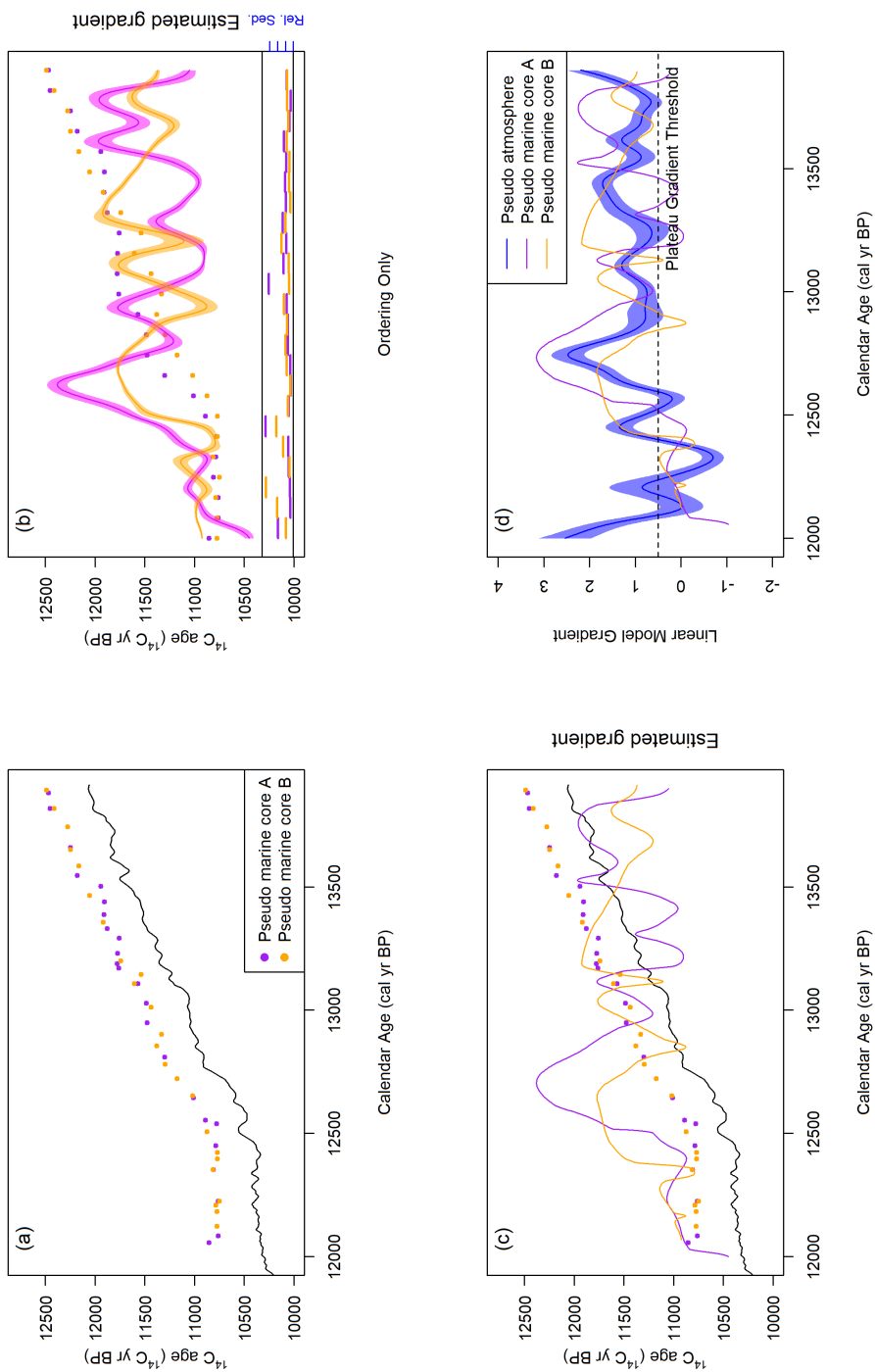


Figure 6

